The root-knot nematode effector MiMSP32 targets host 12-oxophytodienoate reductase 2 to regulate plant susceptibility

Ava Verhoeven[1,2,3] (iD), Anna Finkers-Tomczak[1] (iD), Pjotr Prins[1] (iD), Debbie R. Valkenburg-van Raaij[1], Casper C. van Schaik[1], Hein Overmars[1] (iD), Joris J. M. van Steenbrugge[1] (iD), Wannes Tacken[1], Koen Varossieau[1], Erik J. Slootweg[1] (iD), Iris F. Kappers[4] (iD), Michaël Quentin[5] (iD), Aska Goverse[1] (iD), Mark G. Sterken[1] (iD) and Geert Smant[1] (iD)

[1]Laboratory of Nematology, Department of Plant Sciences, Wageningen University & Research, Droevendaalsesteeg 1, 6708 PB, Wageningen, the Netherlands; [2]Plant Stress Resilience, Utrecht University, Padualaan 8, 3584 CH, Utrecht, the Netherlands; [3]Plant-Environment Signaling, Utrecht University, Padualaan 8, 3584 CH, Utrecht, the Netherlands; [4]Laboratory of Plant Physiology, Department of Plant Sciences, Wageningen University & Research, Droevendaalsesteeg 1, 6708 PB, Wageningen, the Netherlands; [5]INRAE, Université Côte d'Azur, CNRS, ISA, F-06903, Sophia Antipolis, France

Summary

• To establish persistent infections in host plants, herbivorous invaders, such as root-knot nematodes, must rely on effectors for suppressing damage-induced jasmonate-dependent host defenses. However, at present, the effector mechanisms targeting the biosynthesis of biologically active jasmonates to avoid adverse host responses are unknown.

• Using yeast two-hybrid, *in planta* co-immunoprecipitation, and mutant analyses, we identified 12-oxophytodienoate reductase 2 (OPR2) as an important host target of the stylet-secreted effector MiMSP32 of the root-knot nematode *Meloidogyne incognita*. MiMSP32 has no informative sequence similarities with other functionally annotated genes but was selected for the discovery of novel effector mechanisms based on evidence of positive, diversifying selection.

• OPR2 catalyzes the conversion of a derivative of 12-oxophytodienoate to jasmonic acid (JA) and operates parallel to 12-oxophytodienoate reductase 3 (OPR3), which controls the main pathway in the biosynthesis of jasmonates. We show that MiMSP32 targets OPR2 to promote parasitism of *M. incognita* in host plants independent of OPR3-mediated JA biosynthesis.

• Artificially manipulating the conversion of the 12-oxophytodienoate by OPRs increases susceptibility to multiple unrelated plant invaders. Our study is the first to shed light on a novel effector mechanism targeting this process to regulate the susceptibility of host plants.

Introduction

The tropical root-knot nematode *Meloidogyne incognita* ranks high on the list of most invasive plant disease-causing agents world-wide (Bebber *et al.*, 2014). This polyphagous plant parasite feeds on both monocots and dicots, including not only many important food crops, but also the model plant Arabidopsis (Sijmons *et al.*, 1991). After penetrating the root epidermis, infective second-stage juveniles (J2) of *M. incognita* migrate through the cortex and the root apical meristem to enter the host vascular cylinder, where they induce several permanent feeding cells (Wyss & Grundler, 1992; Williamson & Gleason, 2003; Abad & Williamson, 2010). These so-called giant cells are multinucleate and hypertrophied plant cells, which can reach up to 100 times the size of a normal vascular parenchyma cell (Kyndt *et al.*, 2013). Plant-feeding juveniles of *M. incognita* selectively extract assimilates from the

cytoplasm of giant cells with their protrusible oral stylet. Over a period of several weeks, while intermittently feeding on different giant cells, the juveniles of *M. incognita* develop through successive molts into mature females, which produce offspring as egg masses on the root surface (Gheysen & Mitchum, 2019).

The biosynthesis of jasmonates is thought to be important for orchestrating damage-induced host responses to root-knot nematodes in plants (Gheysen & Mitchum, 2019). The first phase of jasmonate biosynthesis occurs in plastids, where lipid-derived linoleic and linolenic acids are converted into 12-oxophytodienoic acid (12-OPDA) by 13-lipoxygenases (LOXs), allene oxide synthases (AOS), and allene oxide cyclases. It has been shown that the mutant tomato *spr2*, which is defective in the conversion of linoleic acid to linolenic acid (Li *et al.*, 2003), is much more susceptible to *M. incognita* than wild-type plants (Fan *et al.*, 2015; Wang *et al.*, 2019).

Likewise, disrupting the 13-lipoxygenase genes *LOX3* and *LOX4* in Arabidopsis alters host susceptibility to *Meloidogyne javanica* infections (Ozalvo *et al.*, 2014). Further downstream, the Arabidopsis mutant, *dde2* mutant lacking an allene oxide synthase required for jasmonate biosynthesis, is more susceptible to *Meloidogyne hapla* (Gleason *et al.*, 2016). The *hebiba* rice mutant, which is defective in an allene oxide cyclase (Riemann *et al.*, 2013), also shows increased susceptibility to *Meloidogyne graminicola* (Nahar *et al.*, 2011). After its transport to peroxisomes, 12-oxophytodienoate reductase 3 (OPR3) catalyzes the conversion of 12-OPDA to jasmonic acid (JA), which is then released into the cytosol. Surprisingly, the Arabidopsis 12-oxophytodienoate reductase 3 mutant *opr3* shows no difference in susceptibility to *M. hapla* as compared to wild-type Arabidopsis plants, suggesting that OPDA – but not JA – might regulate host susceptibility to root-knot nematodes (Gleason *et al.*, 2016). However, more recent studies suggest that 12-OPDA derivatives can also be reduced to JA via an alternative pathway, which takes place in the cytosol, and which is catalyzed by 12-oxophytodienoate reductase 2 (OPR2; Chini *et al.*, 2018). Cytosolic JA can subsequently be converted into biologically active JA-isoleucine (JA-Ile) in a reaction catalyzed by jasmonyl isoleucine synthetase (JAR1). In line with other jasmonate biosynthesis mutants, *jar1-1* knockout mutant rice plants display increased susceptibility to *M. graminicola* (Singh *et al.*, 2020). Altogether, these findings illustrate that interfering in the biosynthesis of jasmonates can enhance the susceptibility of host plants to root-knot nematodes.

Meloidogyne incognita secretes a plethora of effectors to manipulate host development and defenses (Mitchum *et al.*, 2013). Most of these effectors are produced in three pharyngeal glands, which are large single-celled specialized secretory glands that are connected via the pharyngeal lumen to the basal opening of the oral stylet. By salivation through the oral stylet, *M. incognita* delivers effectors into the apoplast or cytoplasm of host cells, where they interact with host targets to promote parasitism (Hussey, 1989; Mejias *et al.*, 2019). Several studies suggest that root-knot nematodes utilize effectors to target damage-induced jasmonate biosynthesis and/or signaling. For instance, ectopic expression of the *M. incognita* effectors MiISE5 and MiSE6 in Arabidopsis changes the transcriptional regulation of multiple JA signaling genes (Shi *et al.*, 2018a,b). Similarly, the expression of the *M. javanica* effector Mj2GO2 in transgenic Arabidopsis affects the regulation of genes associated with JA-mediated plant responses, as well as constitutive levels of JA-Ile (Song *et al.*, 2021). However, at present, the host targets and mode of action of root-knot nematode effectors interfering in the biosynthesis and signaling of jasmonates are unknown.

Currently, the number of candidate nematode effectors generated by whole-genome sequencing exceeds by far the capacity to establish which of the candidates are bona fide effectors (Nguyen *et al.*, 2018; Shukla *et al.*, 2018). Prior work with other plant parasitic nematodes suggests that effector families involved in the activation and suppression of host defense are prone to mutations and recombination (and subsequent diversifying selection; Carpentier *et al.*, 2012; Pokhare *et al.*, 2020).

For this study, we used evidence of positive diversifying selection to prioritize the effector candidate MiMSP32 of *M. incognita* for the further functional characterization *in planta* (Baskaran *et al.*, 2017). We investigated the importance of MiMSP32 for the parasitism of *M. incognita* using host-induced gene silencing and effector overexpression in transgenic tomato plants. To identify the host targets of MiMSP32 in tomato and Arabidopsis, we screened a yeast two-hybrid (Y2H) library of nematode-infected tomato roots and confirmed candidate interactors by *in planta* co-immunoprecipitation. After assessing the susceptibility of Arabidopsis knockout mutants of the candidate host interactors of MiMPS32, we could conclude that this effector targets 12-oxophytodienoate reductase 2 (OPR2) to regulate host susceptibility. AtOPR2 has been shown to catalyze the conversion of 4,5-didehydro-jasmonate (4,5-ddh-JA), a derivative of 12-OPDA, to JA (Chini *et al.*, 2018). Taken together, our data provide the first evidence of a nematode effector regulating host susceptibility by targeting an enzyme in the biosynthesis of jasmonates in plants.

Materials and Methods

Evidence of positive, diversifying selection in MiMSPs

To first test which of the 27 previously identified pioneer MiMSP genes (Abad *et al.*, 2008) have homologs in current genome assemblies of *M. incognita* (Kofoid & White, 1919) and other root-knot nematodes, we used their predicted mRNA sequence to query the Wormbase Parasite cDNA database with the BLASTN algorithm (at parasite.wormbase.org, accessed in May 2020). Hits with a BLASTN score below 100 were disregarded as being false positives. The genome assemblies of the root-knot nematodes referred to in this analysis are available at NCBI under the following accession codes: PRJEB8714 dataset for *Meloidogyne arenaria*, *M. incognita*, and *M. javanica* (Blanc-Mathieu *et al.*, 2017); the PRJNA340324 dataset for *M. arenaria*, *Meloidogyne enterolobii*, *Meloidogyne floridensis*, *M. incognita*, and *M. javanica* (Szitenberg *et al.*, 2017); the PRJNA438575 dataset for *M. arenaria* (Sato *et al.*, 2018); the PRJEB6016 dataset version nMf.1.0 from nematodes.org for *M. floridensis*; and the PRJNA29083 dataset for *M. hapla* (Opperman *et al.*, 2008).

For MiMSPs with three or more hits in the genome assembly of *M. incognita* PRJEB8714, we generated a multiple sequence alignment of the coding sequences of the paralogous genes using CLUSTALW2. The resulting alignment was used to construct a cluster tree based on the Tamura-Nei genetic distance model. MiMSPs with three or more paralogs in the PRJEB8714 genome assembly of *M. incognita* were also tested for signatures of positive selection using the CODEML algorithm of PAML 4.7 (phylogenetic analysis by maximum likelihood; Yang, 1997, 2007; Yang & Bielawski, 2000) within EASYCODEML v.1.21 (Gao *et al.*, 2019). As input files, we used the aligned coding sequences of the MiMSPs paralogs, and an accompanying neighbor-joining tree generated under the Tamura-Nei genetic distance model. EASYCODEML was run under the preset mode for nested models using default settings to compare site models M7 vs M8. Significance was

calculated using log-likelihood ratio tests for the full model comparisons with an alpha of 0.05.

Nematode infection assays

Nematode preparation and sterilization *Meloidogyne incognita* eggs (strain 'Morelos' from INRA, Sophia Antipolis, France) were obtained from infected tomato plants (*Solanum lycopersicum* L. cv MoneyMaker) as described previously (Warmerdam *et al.*, 2018). In short, roots of infected tomato plants were rinsed in water to remove sand particles 10 wk after inoculation and eggs were extracted by incubation in 0.05% (v/v) bleach for 3 min followed by sieving (Hussey & Barker, 1973). Eggs were disinfected using 0.02% sodium azide (NaN) for 20 min and washed thoroughly with tap water. Hatching took place at room temperature in the dark on a 25 μm hatching sieve with 1.5 mg ml^{-1} gentamycin and 0.05 mg ml^{-1} nystatin. After 4 d, J2s were collected by separation on a 70% sucrose column and sterilized by incubation for 10 min in 0.002% (v/v) Triton X-100, 0.004% (w/v) NaN, and 0.004% (w/v) mercury chloride. After surface sterilization, nematodes were rinsed in sterile tap water three times before use and transferred to a 0.7% (w/v) Gelrite solution (Duchefa Biochemie, Haarlem, the Netherlands).

Infection assays on tomato For *in vitro* infection assays, tomato seeds (*S. lycopersicum* L. cv MoneyMaker, or the same cultivar with MiMSP32^{-sp}-derived plasmids; Supporting Information Methods S1, S2) were first incubated for 3 d in tap water at 4°C in the dark. Thereafter, the seeds were briefly washed with 70% ethanol and 2.5% (v/v) bleach and incubated three times for 10 min in sterile tap water. Batches of seeds were sowed on square plates of 10 cm containing ½ MS20 medium (2.35 g l^{-1} Murashige & Skoog (MS) with vitamins (Duchefa Biochemie), 20 g l^{-1} sucrose, pH 6.4, 7.0 g l^{-1} Gelrite (Duchefa Biochemie)). After incubating for 4 d at 24°C in 16 h : 8 h, light : dark, germinated plants were transferred to fresh square plates containing ½ MS20 medium. The transferred plants were allowed to grow for an additional 6 d under the same conditions, after which they were inoculated with 120 infective *M. incognita* J2s per plant. Plants were kept horizontally in the dark for 2 d at 24°C, after which they were placed diagonally in 16 h : 8 h, light : dark conditions again. To reduce the direct exposure of the roots to light, the bottom 8 cm of the plates was covered with paper sleeves. Seven days postinoculation (dpi), the number of galls formed in the roots was counted by visually inspecting the roots with a dissection microscope.

Infection assays on Arabidopsis Arabidopsis seeds (*Arabidopsis thaliana* (L.) Heynh. accession Col-0 (CS60000), or mutants mentioned later) were vapor-sterilized for 4 h in 0.7 M sodium hypochlorite and 1% hydrogen chloride before sowing in plates containing MS20 medium (4.7 g l^{-1} MS with vitamins (Duchefa Biochemie), 20 g l^{-1} sucrose, pH 6.4, 0.7% Gelrite (Duchefa Biochemie)). Seeds were stratified for at least 3 d at 4°C. Arabidopsis seeds were stimulated to germinate at 24°C under a 16 h : 8 h, light : dark regime. After 6 d, individual plants were transferred to fresh six-well culture plates and allowed to grow and settle for an additional 7 d, after which they were inoculated with 180 infective J2s of *M. incognita* per plant. A slightly higher amount of J2s per plant was used to ensure a comparable infection pressure, because of the susceptibility differences in between tomato and Arabidopsis. Nematode-containing 6-well plates were incubated at 24°C under dark conditions for the duration of the bioassay.

Data collection and statistical analysis The number of root tips was counted for each plant at the time of inoculation. Data were collected in at least three independent experiments and pooled for statistical analysis and visualization. The number of nematodes inside the roots was counted at 7 dpi by means of acid fuchsin staining on the whole root system. Therefore, clean roots were incubated for 5 min in 2.5% household bleach followed by rinsing for 10 min in tap water. Next, roots were incubated in fuchsin-staining solution (0.2 M acid fuchsin and 0.8% glacial acetic acid in tap water) for 30 s in a microwave oven at maximum power. Finally, roots were transferred to 40% glycerol and nematodes could be counted visually using a dissection microscope.

Counting data from tomato or Arabidopsis were collected in at least two independent experiments with $n \geq 16$ and combined for statistical analysis and visualization. To be able to pool the data of independent experiments, we normalized the counts for batch effects (Fig. S1d). To this end, the actual counts were corrected based on the average of counts on wild-type plants from a single independent experiment against the average of counts on wild-type plants over all experiments using

$$T_{norm} = T_i - (\overline{T}_{i,\text{Col}-0} - \overline{T}_{\text{total},Col-0})$$

where T_{norm} is the normalized number of nematodes or nematode-induced galls, i is the individual experiment, and $\overline{T}$ is the averaged number.

The batch-corrected data for nematode numbers, gall numbers, and root tip numbers were analyzed in R v.3.6.1. x64. Extreme outliers in the dataset outside the interquartile range of 1.5 were removed (Vinutha *et al.*, 2018). Normality was checked using *qq*-plots from the GGPUBR package, and statistical comparison was done using either an ANOVA analysis with *post hoc* Tukey's HSD or Student's *t*-tests, depending on the number of treatments or plant lines. Data visualization was done using the GGPLOT2 package (Wickham, 2016).

Yeast two-hybrid screen

A yeast two-hybrid screen was performed as a custom service using full-length MiMSP32 minus the signal peptide as bait and a cDNA library of infected tomato roots (*S. lycopersicum* L. cv M82) as prey (Hybrigenics Services, Evry, France). This cDNA library was constructed with mRNA from an equal mixture of tomato root tissue infected with *Ralstonia solanacearum* (4-wk-old roots on soil, infected with strain GMI1000 or GMI1694 (hrp−), which were harvested at 12 h postinfection), root tissue infected with *M. incognita* (3-wk old roots (on soil or *in vitro*)) infected with *M. incognita* (galls dissected at 4–5 dpi and 7–8 dpi and whole infected roots 7–8 dpi), and uninfected roots

(1- to 3-wk-old plants grown on soil or *in vitro*), and is available as 'Tomato Roots Infected_RP1' (Hybrigenics Services). Hybrigenics Services performed their optimized ULTImate Y2H™ technique and provided information to separate artifacts from specific interactions by the global predicted biological score (PBS), which is based on a statistical model (Rain *et al.*, 2001). Alignments of individual clone sequences described with both a forward and a reverse sequence were made in GENEIOUS v.8.1.9 (Biomatters, Auckland, New Zealand).

Co-immunoprecipitation assays

Transient expression and total protein extraction were done according to Methods S3. Protein extract was first mixed with 50 µl rabbit-IgG agarose (Sigma-Aldrich) and incubated with 50 µl anti-HA microbeads. Co-immunoprecipitation was done with separation columns from µMACS Epitope Tag Protein Isolation Kit (Miltenyi Biotec, Bergisch Gladbach, Germany) according to manufacturer's instructions. Soluble fractions were analyzed by SDS-PAGE on a 12% Bis-Tris gel (Invitrogen), and proteins were subsequently transferred to a PVDF membrane for Western blotting (Thermo Fisher, Waltham, MA, USA). Protein bands were visualized either with a Roche Anti-HA-Peroxidase high affinity from rat IgG1 (Scientific Laboratory Supplies, Wilford, UK) or with a primary goat anti-MYC antibody (Abcam, Cambridge, UK) and a horseradish peroxidase-conjugated secondary antibody of donkey anti-goat (Jackson ImmunoResearch, Ely, UK). SuperSignal West 1 : 1 Femto-Dura Substrate (Thermo Fisher) was used to detect horseradish peroxidase-conjugated antibodies in the G:BOX Chemi System (Syngene, Bangalore, India). To confirm equal protein loading, membranes were also stained with Coomassie brilliant blue.

Subcellular localization using confocal microscopy

To assess the subcellular localization of MiMSP32^{-SP} without its signal peptide for secretion, and with and without the putative interacting host protein fragments in plant cells, the proteins were transiently expressed by agroinfiltration in *Nicotiana benthamiana* epidermal cells (Methods S3). Agroinfiltrated leaves overexpressing either HA4_GFP_MiMSP32^{-SP} or MiMSP32^{-SP}_GFP_HA4 in combination with the interacting domain of possible interactors (SID) in MYC4_mCh_SID or SID_mCh_MYC4 configuration, or with free mCherry, were collected for microscopic observations with a Zeiss LSM 510 Confocal Microscope (Carl Zeiss). For imaging of constructs carrying a GFP tag, the 488 nm line of an argon-ion laser was used for excitation and GFP emission was selected through a band-pass filter of 505–530 nm for detection. For constructs carrying a mCherry tag, imaging was done using a 543 nm HeNe laser for excitation and mCherry emission was selected by a 600–650 nm band-pass filter. Chlorophyll emission was detected using a 650 nm long-pass filter. Images were equally enhanced in brightness for publication in print.

To quantify differences in subcellular localization, the ratios in fluorescence intensity between cytoplasm and nucleus were calculated in IMAGEJ. Normality of the data was checked using *qq*-plots from the GGPUBR package in R v.3.6.1 x64, and a one-way ANOVA with *post hoc* Tukey's HSD was used to determine statistical differences.

Arabidopsis mutant genotyping

Arabidopsis seeds were obtained from the European Arabidopsis Stock (Alonso *et al.*, 2003) of T-DNA mutant lines of the following genes: At5g04930; SALK_002106C (*ala1-1*) and SALK_056947C (*ala1-2*), At1g76690C; SALK_116381C (*opr2-1*), and At4g20850; -SALK_085776C (*tppII-2*). Additionally, the Saskatoon insertion line *opr3-3* (SK24765; Robinson *et al.*, 2009) and *opr2-1/opr3-3* double mutants were provided by Chini *et al.* (2018). All above-mentioned plant lines are in the same Arabidopsis Col-0 (N60000) genetic background, which was also used as a wild-type control in our experiments. Seeds were propagated by selfing and MeJA addition for the *opr3-3* and *opr2-1/opr3-3* mutant lines as described previously (Chini *et al.*, 2018). Homozygosity of selected T-DNA insertion lines was confirmed by PCR (Fig. S2) using primer pairs WT1 : M5 (Table S1). Homozygosity of *opr2-1*, *opr3-3*, and *opr2-1/opr3-3* insertion lines without cross-contamination was confirmed by PCR (Fig. S3; see primer pairs WT3, M3, WT6 and M6 in Table S1). All plant lines contained the correct insertions.

Results

Evidence of positive selection in putative *M. incognita* effectors

Twelve years after the publication of the first *M. incognita* genome sequence (Abad *et al.*, 2008), we revisited the status of 27 previously identified 'pioneer genes' isolated from gland-specific cDNA libraries by Huang *et al.* (2003) using the latest root-knot nematode genome assemblies available (Blanc-Mathieu *et al.*, 2017). Querying the WormBase ParaSite nucleotide sequence database with these 27 genes, hereafter named MiMSPs, yielded significantly matching sequences from one or more root-knot nematode species (Fig. 1a). Surprisingly, for only 19 MiMSPs originally identified in *M. incognita*, we found at least one significantly matching gene prediction in the latest genome assembly of *M. incognita* (Meloidogyne_incognita_V3; Fig. 1b). Furthermore, for eight MiMSPs, we found an overlap in the matching gene predictions, because of high similarity in the MiMSP query sequences. For six MiMSPs, we identified three or more paralogs in the genome of *M. incognita* (Fig. 1b,c), which could be further tested for evidence of positive selection using CODEML algorithm of PAML (phylogenetic analysis by maximum likelihood; Yang, 1997, 2007; Yang & Bielawski, 2000). The log-likelihood ratio tests of the nonsynonymous over synonymous mutation rates for three MiMSP (i.e. MiMSP17, MiMSP31, and MiMSP32) significantly favored codon substitution model M8, which does allow for positive selection, over M7, which does not allow for positive selection (Table S2; Fig. 1c). We therefore concluded that these three MiMSPs represent
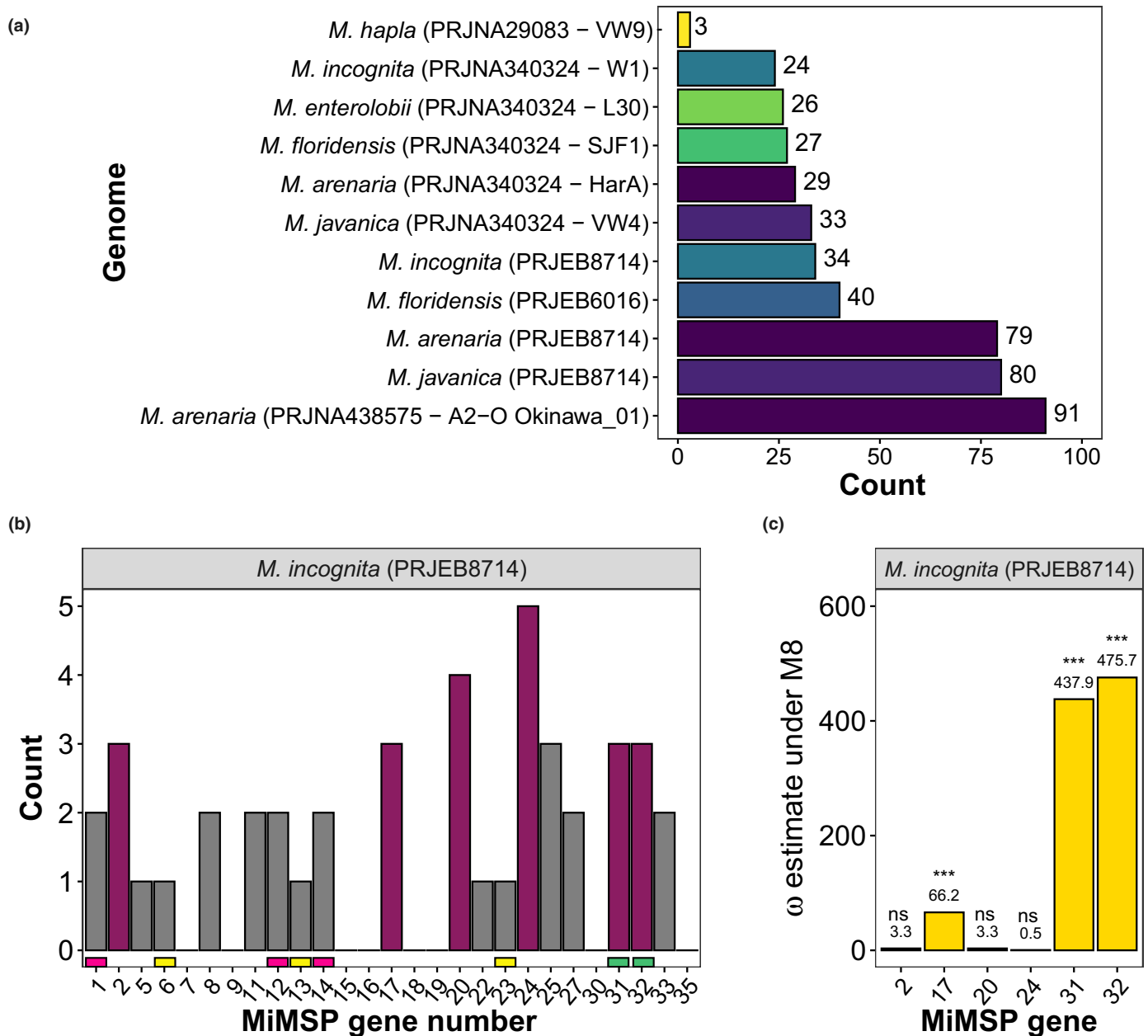
Fig. 1 MiMSP17, MiMSP31, and MiMSP32 are under positive diversifying selection. (a) The number of significantly matching genes within all published assemblies of root-knot nematode genomes in the WormBase ParaSite database queried with 27 MiMSPs using BLASTN. Colors indicate nematode species. (b) The number of significantly matching genes for each specific MiMSP in the *Meloidogyne incognita* PRJEB8714 genome sequence. MiMSPs with three or more paralogous genes in the *M. incognita* genome are indicated in purple. Small colored rectangles below the bars indicate identical hits caused by high sequence similarity in MiMSP query. (c) Estimated nonsynonymous/synonymous substitutions rates (omega) for six clusters of MiMSP paralogs. In yellow, MiMSP genes with clusters of paralogs for which the log-likelihood ratio test significantly favored model M8 for positive selection (***, $P < 0.0001$; ns, not significant).

clusters of positively selected paralogous genes in the genome of *M. incognita*.

As the estimated ω under model M8 for positive selection for MiMSP31 and MiMSP32 proved to be much larger than for MiMSP17 (Fig. 1c), we initially focused our analyses on these two genes. Prior work has shown that MiMSP31 and MiMSP32 encode putative secretory proteins specifically localized in the dorsal pharyngeal gland of parasitic J2s and later stages in *M. incognita* (Huang *et al.*, 2003). However, closer inspection revealed that

MiMSP31 has a high sequence similarity with 150 residues at the amino terminus of MiMSP32 (Fig. S4), and both are likely splice variants of the same transcript. We therefore chose to focus further on the functional characterization of MiMSP32. An initial protein sequence analyses of MiMSP32 revealed no specific motifs, structures, or domains, confirming its classification as 'pioneering gene'. However, we noted that the three paralogous genes of MiMSP32 in the *M. incognita* genome, called Minc3s00381g11350, Minc3s00827g17824, and Minc3s00593g14814, are classified as

putative UDP-glycosyltransferases (IPR002213) by INTERPROSCAN (Blum *et al.*, 2021).

MiMSP32 functions as a bona fide effector

To investigate whether MiMSP32 promotes parasitism by *M. incognita* in tomato, we first used host-induced gene silencing with a hairpin construct targeting nucleotides 313–522 of the MiMSP32 transcript (Fig. 2a). At 7 dpi, we observed a significantly lower number of nematode-induced galls for two independently transformed tomato lines (Methods S1, S2, S4; Fig. S1a) overexpressing the pSMD:MiMSP32_hp hairpin construct compared with wild-type tomato plants (Fig. 2b).

Next, we tested whether ectopic overexpression of MiMSP32 alters the susceptibility of tomato plants to *M. incognita*. We challenged seedlings of two independently transformed tomato lines overexpressing MiMSP32 without its native signal peptide with infective J2 in an *in vitro* bioassay (Methods S1, S2, S4; Fig. S1b,c). At 7 dpi, we observed a significant increase in the number of galls in roots of the two tomato lines overexpressing MiMSP32 as compared to wild-type tomato plants (Fig. 2c). Based on the plant phenotypes of our gene silencing and overexpression constructs, we concluded that MiMSP32 functions as *bona fide* effector for *M. incognita* promoting nematode parasitism in roots of tomato plants.

MiMSP32 interacts with SlOPR2

To identify host targets of MiMSP32 in tomato, we screened a Y2H cDNA library made of nematode-infected tomato roots (i.e.

galls from 4 to 5 and 7 to 8 dpi, and whole root systems from 7 to 8 dpi) using MiMSP32 without its native signal peptide as bait. In total, 127 million yeast colonies were analyzed, resulting in the identification of 51 tomato protein fragments possibly interacting with MiMSP32 (Table S3). Next, we ranked these tomato protein fragments according to the calculated level of confidence for their interactions with MiMSP32 using a PBS (Formstecher *et al.*, 2005). Based on this score, we selected 11 probable interactors of MiMSP32, six of which with high confidence (Table S4). The number of unique independent positive yeast clones for each of the probable interactors of MiMSP32 ranged from 4 to 20. Aligning the clone inserts with the best matching predicted full-length proteins in sequence database of tomato genome version SL2.50 enabled us to identify the six corresponding genes as Solyc06g073580.2.1 (SlH6D; hyoscyamine 6-dioxygenase), Solyc10g074940.1.1 (SlALA1; phospholipid-transporting ATPase 1-like), Solyc12g010040.1.1 (SlLAPA2; leucine aminopeptidase), Solyc01g103390.2.1 (SlOPR2; oxo-phytodienoate reductase 2), Solyc03g025610.1.1 (SlTPPII; tripeptidyl-peptidase 2), and Solyc10g081020.1.1 (SlSTP6; transcription elongation factor SPT6-like) (Table S5).

Next, we analyzed predicted physiochemical properties of the six interacting protein fragments that could result in nonspecific binding in the Y2H screen (Table S6). We also determined the positions of the interacting fragments relative to predicted subcellular localization signals and conserved protein motifs and domains in the matching full-length proteins (Marchler-Bauer *et al.*, 2016). For SlOPR2 (Fig. 3a), the minimal interacting fragment contains nine out of 14 active sites, including substrate binding sites and flavin mononucleotide binding sites. For
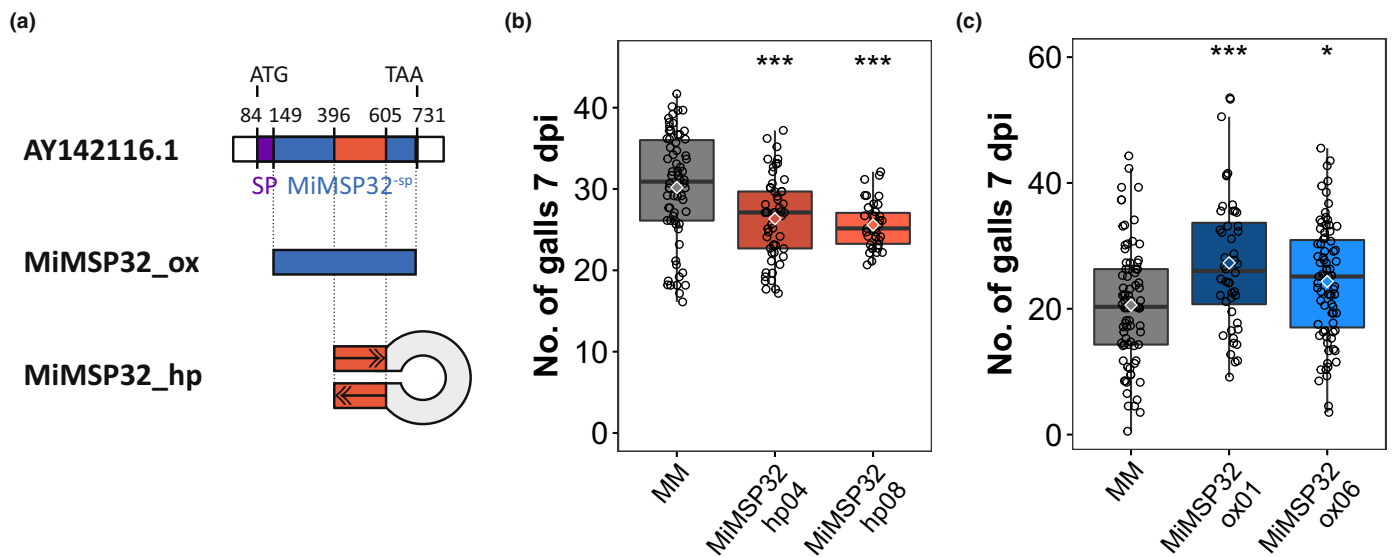
Fig. 2 MiMSP32 promotes *Meloidogyne incognita* parasitism in tomato. (a) The target sequence in MiMSP32 for host-induced gene silencing using hairpin construct MiMSP32_hp. AY142116.1 refers to the GenBank accession number of the MiMSP32 mRNA sequence. (b) Number of galls per plant at 7 d postinoculation (dpi) with *M. incognita* on two independent tomato lines overexpressing the hairpin construct MiMSP32_hp (MiMSP32_hp04 and MiMSP32_hp08) and wild-type tomato plants (MM). (c) Number of galls per plant on two independent tomato lines overexpressing MiMSP32 coding sequence (MiMSP32_ox01 and MiMSP32_ox06) without the predicted signal peptide for secretion and wild-type tomato plants (MM) at 7 dpi with *M. incognita*. Data were collected in multiple independent experiments, batch-corrected, and combined for statistical analysis with a one-way ANOVA. Boxplots represent the minimum, first quantile, median, third quantile, and maximum. The diamond shape represents the average value, and the circles represent all individual measurements. Asterisks indicate significant differences between transgenic lines and wild-type tomato (as calculated with a one-way ANOVA and Tukey's HSD): *, $P < 0.05$; ***, $P < 0.001$.

SlSPT6 (Fig. S5), the interacting fragment contains one of the four nuclear localization sites, while the other three are located outside the interacting fragment. However, we could not find any structural properties in the proteins to help us prioritize the probable interacting fragments for further studies *in planta*.

We therefore proceeded to independently confirm interactions of MiMSP32 with all six probable host targets by co-expressing affinity-tagged constructs of the selected interaction domains of the interactors with pBIN:MiMSP32^{-sp}_GFP_HA4 (Methods S5) in *N. benthamiana* Domin leaves. Co-immunoprecipitation with anti-HA magnetic beads showed that five out of six putative interactor fragments (Methods S6) also specifically bind to MiMSP32^{-sp}_GFP_HA4 in plant cells (e.g. SlOPR2 in Figs 3b, S6). In addition, we used the same constructs to observe the induction of a possible shift in subcellular localization of these interacting fragments *in planta* by co-expression with MiMSP32^{-sp} (Fig. S7a,b). We reasoned that binding to a probable interactor might shift the subcellular localization of MiMSP32 toward the localization of its interactor, or *vice versa*. To test this, we transiently co-expressed GFP-tagged MiMSP32^{-sp} with the putative interactor domain fused with mCherry in *N. benthamiana* (e.g. SlOPR2^{SID} in Fig. 3c). When expressed alone, MiMSP32 has a similar fluorescence intensity in nucleus and cytoplasm. Interestingly, we noticed a significant shift in subcellular localization of MiMSP32^{-sp}_GFP_HA4 toward the cytoplasm when it was co-expressed with three out of six putative interactor fragments (e.g. SlOPR2^{SID} in Figs 3d, S7c). The shift in subcellular localization of SlALA1^{SID} was statistically not significant, yet visually evident. Taking the data of the co-immunoprecipitation experiments and shifts in the subcellular localization together, we conclude that MiMSP32 interacts *in planta* with fragments of the tomato proteins phospholipid-transporting ATPase 1-like (SlALA1), leucine aminopeptidase (SlLAPA2), oxophytodienoate reductase 2 (SlOPR2), and tripeptidyl-peptidase 2 (SlTPPII).

The MiMSP32 target AtOPR2 regulates the susceptibility of Arabidopsis to *M. incognita*

To test whether the Arabidopsis orthologs of the possible host targets of MiMSP32 play a role in plant susceptibility to root-knot nematodes, we performed nematode bioassays using T-DNA knockout mutants of AtALA1 (*ala1-1* and *ala1-2*), AtOPR2 (*opr2-1*), and AtTPPII (*tppII-1*). The stress-inducible acidic leucine aminopeptidase 2 (SlLAPA2) is thus far only found in a subset of the Solanaceae (Scranton *et al.*, 2012), and therefore, no T-DNA knockout mutant line of a close ortholog of this gene is available for Arabidopsis. In all four knockout mutants, the T-DNA inserts are in gene exons and proved to be homozygous for the insertion (Figs 4a, S2). In multiple independently repeated experiments, only *opr2-1* mutant plants harbored a significantly higher number of nematodes per plant at 7 dpi than wild-type Col-0 plants (Fig. 4b). Taken together, our data of the Arabidopsis mutants suggest that *M. incognita* could enhance host susceptibility by targeting OPR2, and we therefore focused our study further on OPR2.

We first assessed whether MiMSP32 also physically interacts with full-length Arabidopsis AtOPR2 by transiently co-expressing affinity-tagged constructs encoding AtOPR2 and MiMSP32 without its native signal peptide (MiMSP32^{-sp}) in *N. benthamiana* leaves via agroinfiltration. We used MiMSP32^{-sp} fused to GFP- and 4xHA-tags on either N- or C-terminus of the protein and AtOPR2 carrying C-terminal mCherry- and 4xMYC-tags. Indeed, MiMSP32^{-sp} pulled down AtOPR2 in a co-immunoprecipitation assay using anti-HA magnetic beads (Fig. 4c). Our data thus showed that full-length AtOPR2 also interacts with MiMSP32^{-sp}.

OPR2 directs the root transcriptome toward abiotic and biotic stress responses

To resolve gene networks underlying the enhanced susceptibility of the Arabidopsis *opr2-1* mutant to *M. incognita*, we analyzed differential expression patterns in nematode-infected roots of mutant *opr2-1* and wild-type Col-0 plants at 0, 1, 4, and 7 dpi using RNA sequencing. In total, we analyzed 1624 950 228 reads, of which 95.3% mapped to the TAIR10 *A. thaliana* genome (Lamesch *et al.*, 2011; Table S7; Fig. S8; Methods S7). To identify genes specifically affected by the mutation on separate days after inoculation or in interaction with nematode infection, we used a statistical interaction model for plant genotype and *M. incognita* infection on 1, 4, and 7 dpi (Fig. 5a). We found 13 genes which were differentially regulated in roots of the *opr2-1* mutant lines vs wild-type Col-0 upon infection by *M. incognita* (Fig. 5b; Table S8). As expected, the most affected gene in the *opr2-1* mutant at all three time points in both infected and non-infected roots was *AtOPR2* (Fig. 5c). In addition, 12 other genes showed deviating expression patterns in the *opr2-1* mutant when compared to the wild-type Col-0 line (Table S9). Six of these differentially regulated genes are associated with the response to either biotic or abiotic stress, and one has shown to be directly linked with JA responses. Importantly, we also analyzed the relative expression of all genes included in KEGG module M00113 representing the JA biosynthesis pathway in Arabidopsis (Fig. S9). Here, we observed a minor downregulation of the OPDA reductase *AtOPR1* in nematode-infected roots of the *opr2-1* mutant compared with wild-type plants. In conclusion, the impact of OPR2 on the transcriptome of nematode-infected Arabidopsis roots points at alterations in responses to abiotic and biotic stress.

OPR2 and OPR3 differently affect plant susceptibility to *M. incognita*

AtOPR2 is thought to regulate an AtOPR3-independent pathway in the biosynthesis JA (Fig. 6a; Chini *et al.*, 2018). To test whether the two parallel biosynthesis pathways redundantly affect the susceptibility of Arabidopsis to *M. incognita*, we performed nematode bioassays using *opr2-1*, *opr3-3*, and *op2-1/opr3-3* mutant lines. We first observed that both single-mutant lines, *opr2-1* and *opr3-3*, were equally more susceptible to *M. incognita* than wild-type Arabidopsis plants (Fig. 6b). However, the
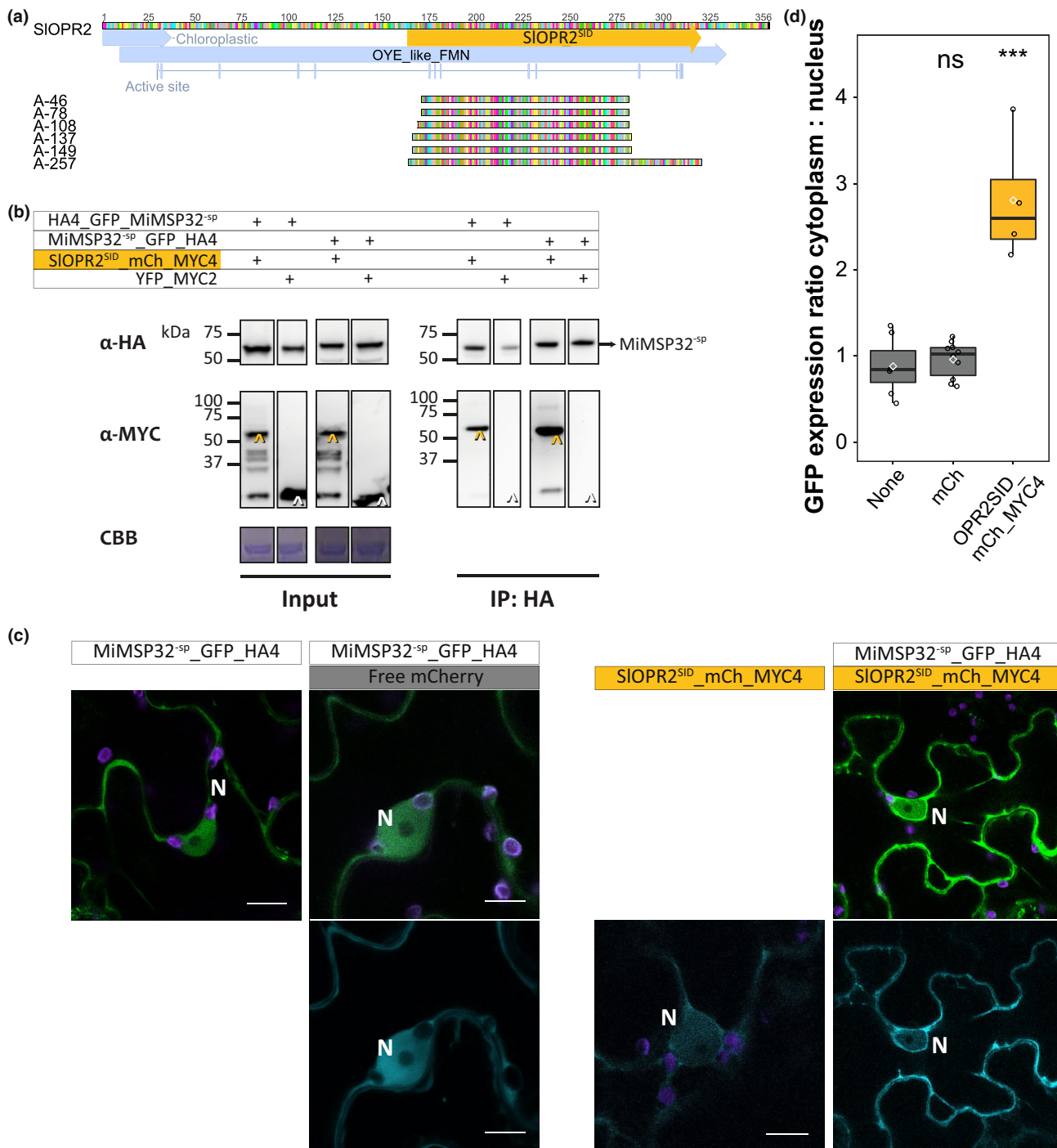
Fig. 3 Protein fragment of the putative host target 12-oxophytodienoate reductase 2 (SlOPR2) interacts with MiMSP32^{-sp} *in planta*. (a) Projection of six independent clones (A-46 to A-257) and the selected interaction domain (SID) from a yeast two-hybrid screen using MiMSP32 as bait on the coding sequence of tomato SlOPR2. (b) Co-immunoprecipitation of HA-tagged MiMSP32^{-sp} and MYC-tagged SlOPR2^{SID} using anti-HA magnetic beads. Equal loading is visualized by Coomassie brilliant blue (CBB) staining on total protein extracts isolated from agroinfiltrated leaves of *Nicotiana benthamiana*. The yellow arrow indicates SlOPR2SID-mCh-MYC4 and the white arrow indicates YFP_MYC2. (c) Subcellular localization of MiMSP32^{-sp}_GFP_HA4 with and without mCherry-tagged SlOPR2^{SID} (right panel) or free mCherry (left panel) in agroinfiltrated leaves of *N. benthamiana*. The confocal pictures represent the mCherry channel (cyan) and the combined GFP channel (green) with chloroplasts (purple). 'N' indicates the position of the nucleus. Bar, 10 μm. (d) The ratio of GFP expression in cytoplasm over nucleus after agroinfiltration in *N. benthamiana* of HA-tagged MiMSP32^{-sp} with SlOPR2SID-mCh-MYC4 (right panel) or mCherry alone (left panel). Statistical analysis was done with a one-way ANOVA and a *post hoc* Tukey HSD. Boxplots represent the minimum, first quantile, median, third quantile and maximum. The diamond shape represents the average value and the circles represent all individual measurements. The horizontal line inside the box represents median. The whiskers mark the values within the first and third quantile. Asterisks indicate significant differences between mCherry-tagged SlOPR2 and MiMSP32^{-sp} without any co-expressed construct: ***, $P < 0.001$; ns, not significant. All leaf samples were taken at 48 h after agroinfiltration of the constructs in *N. benthamiana*.
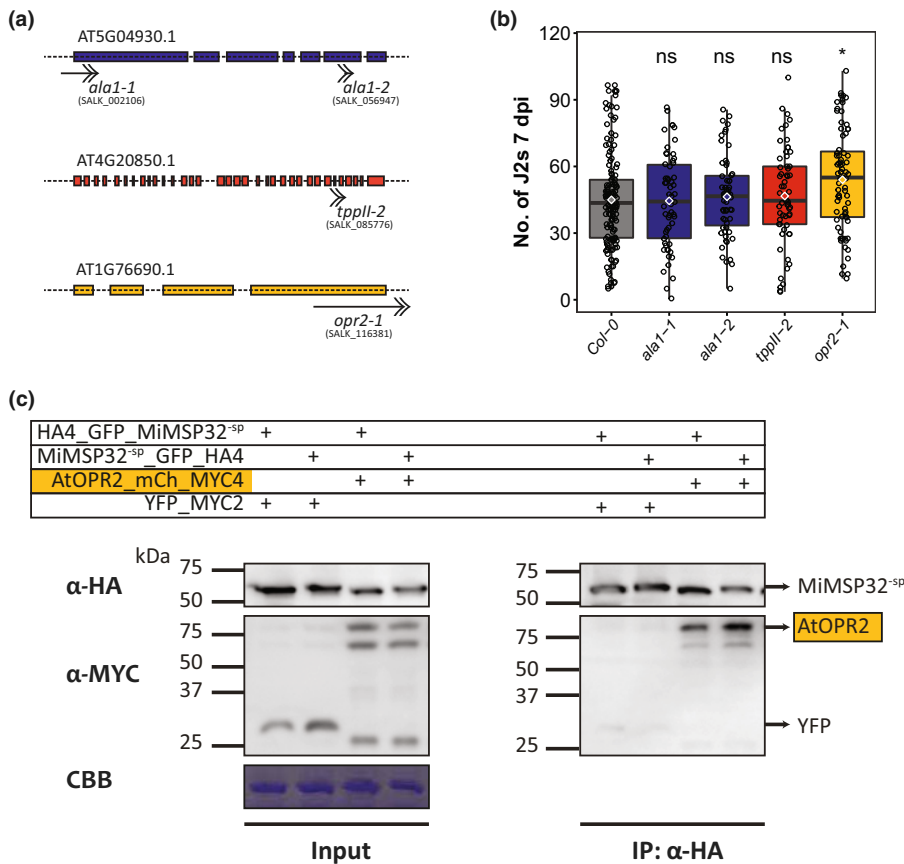
Fig. 4 AtOPR2 is a host target of MiMSP32. (a) Detailed locations of the T-DNA insertions (arrows) in the Arabidopsis mutants *ala1-1*, *ala1-2*, *tppII-1*, and *opr2-1*. (b) Boxplot of the number of acid fuchsin-stained *Meloidogyne incognita* juveniles (J2s) in mutant and wild-type Arabidopsis plants at 7 d postinoculation (dpi). Data were collected in at least three independent experiments with $n \geq 16$, and all data were combined for statistical analysis with ANOVA and Tukey's HSD. Boxplots represent the minimum, first quantile, median, third quantile, and maximum. The diamond shape represents the average value, and the circles represent all individual measurements. Asterisks indicate significant differences between T-DNA lines and wild-type Col-0 Arabidopsis plants: *, $P < 0.05$; ns, not significant. (c) Co-immunoprecipitation in *Nicotiana benthamiana* leaf extracts by pulling down MiMSP32^{-sp} using anti-HA magnetic beads and anti-MYC detection of AtOPR2_mCh_MYC4. Proteins were extracted from multiple leaves and from multiple plants at 48 h after agroinfiltration. Equal loading is visualized by Coomassie brilliant blue (CBB) staining on total protein extracts of agroinfiltrated leaf areas.

double-mutant *opr2-1/opr3-3* was significantly more susceptible than both single mutants, which implies that *opr2-1* and *opr3-3* additively affect the susceptibility of Arabidopsis to *M. incognita*. It has been shown that interfering with OPR3 in the biosynthesis of JA can induce enhanced secondary root formation (Li *et al.*, 2019), which may affect plant susceptibility to root-knot nematodes. Indeed, we also observed a significantly increased root branching phenotype for the single-mutant *opr3-3* at the time of inoculation, but surprisingly not for the *opr2-1* mutant (Fig. 6c). Knocking out *OPR2* on top of *OPR3* in the double-mutant *opr2-1/opr3-3* did not result in a further increase the number of root tips either. This indicates that the parallel pathways independently regulated by OPR2 and OPR3 have different physiological outputs, possibly involving other biologically active compounds.

Targeting of host OPR2 by MiMSP32 may alter 12-OPDA but not JA levels

Next, we tested whether targeting of host OPR2 by the effector MiMSP32 alters the conversion of 12-OPDA into JA in hypersusceptible tomato plants. Hereto, we measured the concentrations of 12-OPDA and JA in the two independent tomato lines constitutively overexpressing MiMSP32 without its native signal peptide for secretion (Methods S8). Notably, the baseline level of 12-OPDA in wild-type tomato plants was extremely low (i.e. below 0.4 fmol per mg fresh weight). Nonetheless, we observed an

increase in the concentration of 12-OPDA in the individual transgenic tomato lines overexpressing MiMSP32, although this was not sufficiently supported in the ANOVA with *post hoc* analysis (Fig. 6d). However, by aggregating the data of the two independent lines, we found a significant effect of the MiMSP32^{-sp}-insertion on the 12-OPDA-concentration in tomato in a t-test (P-value = 0.0039). By contrast, the JA(-Ile) concentrations in the individual transgenic tomato lines overexpressing MiMSP32, or the aggregated data of the two lines, were not significantly different from the wild-type tomato plants. We therefore concluded that MiMSP32 may target OPR2 in host plants to alter the conversion of 12-OPDA without significantly affecting JA-(Ile) levels.

Discussion

Recent developments in sequencing technologies have accelerated the identification of candidate effectors in genomes of plant parasitic nematodes, many of which have no informative homology with functionally annotated genes. The speed at which such novel candidate effectors are currently being identified exceeds the capacity to establish whether they function as *bona fide* nematode effectors *in planta*. Here, we show that evidence of positive, diversifying selection can be used as an additional criterion to prioritize effector candidates for the discovery of novel molecular mechanisms underlying nematode–plant interactions. We demonstrate that the positively selected effector MiMSP32, previously identified as a dorsal pharyngeal gland-specific pioneer gene (named 19F07 in Huang
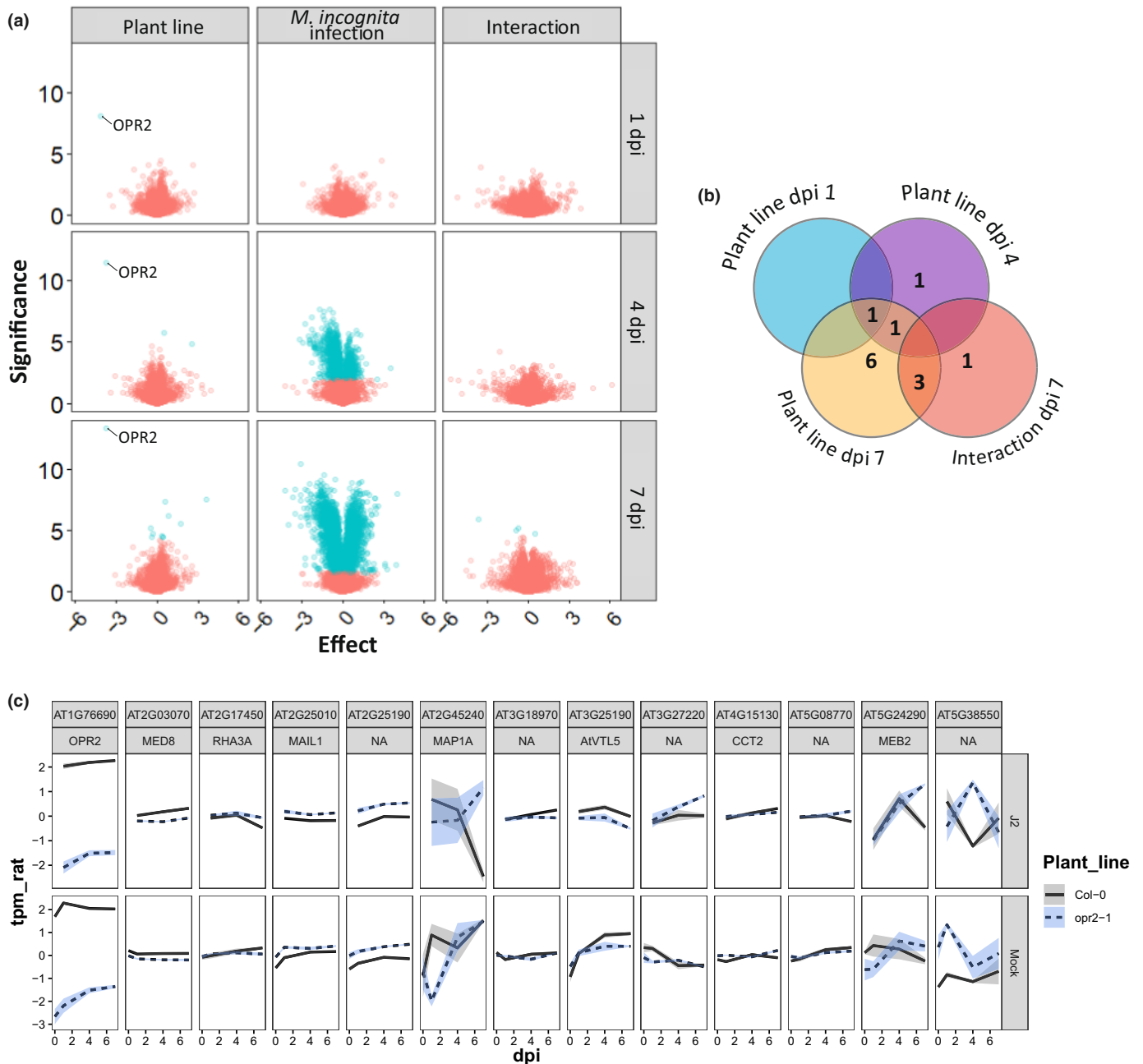
Fig. 5 Thirteen genes are differentially regulated in roots of *Arabidopsis thaliana opr2-1* plants compared with wild-type plants during *Meloidogyne incognita* infection. (a) Volcano plot of differentially regulated genes using interaction model for *opr2-1* and wild-type plants on 1, 4, and 7 d postinoculation (dpi) with *M. incognita* juveniles (J2) or mock-inoculated. Significantly differentially regulated genes (false discovery rate, FDR < 0.05) are colored in blue; nonsignificant differences are colored in red. (b) Venn diagram with the differentially regulated genes, organized by significant factors from the interaction model. (c) Relative expression as the ratio of transcripts per kilobase million (tpm_rat) of the 13 differentially regulated genes at 0, 1, 4, or 7 dpi with *M. incognita* juveniles (J2) or mock-inoculated for the *opr2-1* mutant or Col-0 wild-type plants. The line represents the average and the ribbon the ±SE values. na, not available.

et al., 2003), targets 12-oxophytodienoate reductase 2 (OPR2) in host plants to promote parasitism of *M. incognita*.

As host-induced gene silencing of MiMSP32 in *M. incognita* requires the uptake of dsRNA by feeding, this effector operates most likely in later stages of parasitism after feeding on giant cells has begun. This is in agreement with the temporal expression of MiMSP32 in the dorsal pharyngeal gland of *M. incognita*, which extends from second-stage parasitic juveniles to later parasitic stages (Huang *et al.*, 2003). Our findings also support the hypothesis that dorsal pharyngeal gland-specific effectors of *M. incognita* involved in later stages of parasitism are more likely to be divergent as a consequence of positive selection by different host defense systems (Da Rocha *et al.*, 2021). Indeed, we show that MiMSP32 enhances the susceptibility of host plants to *M. incognita* by targeting an enzyme in the biosynthesis of jasmonates, which play a role in regulating host defenses. However,
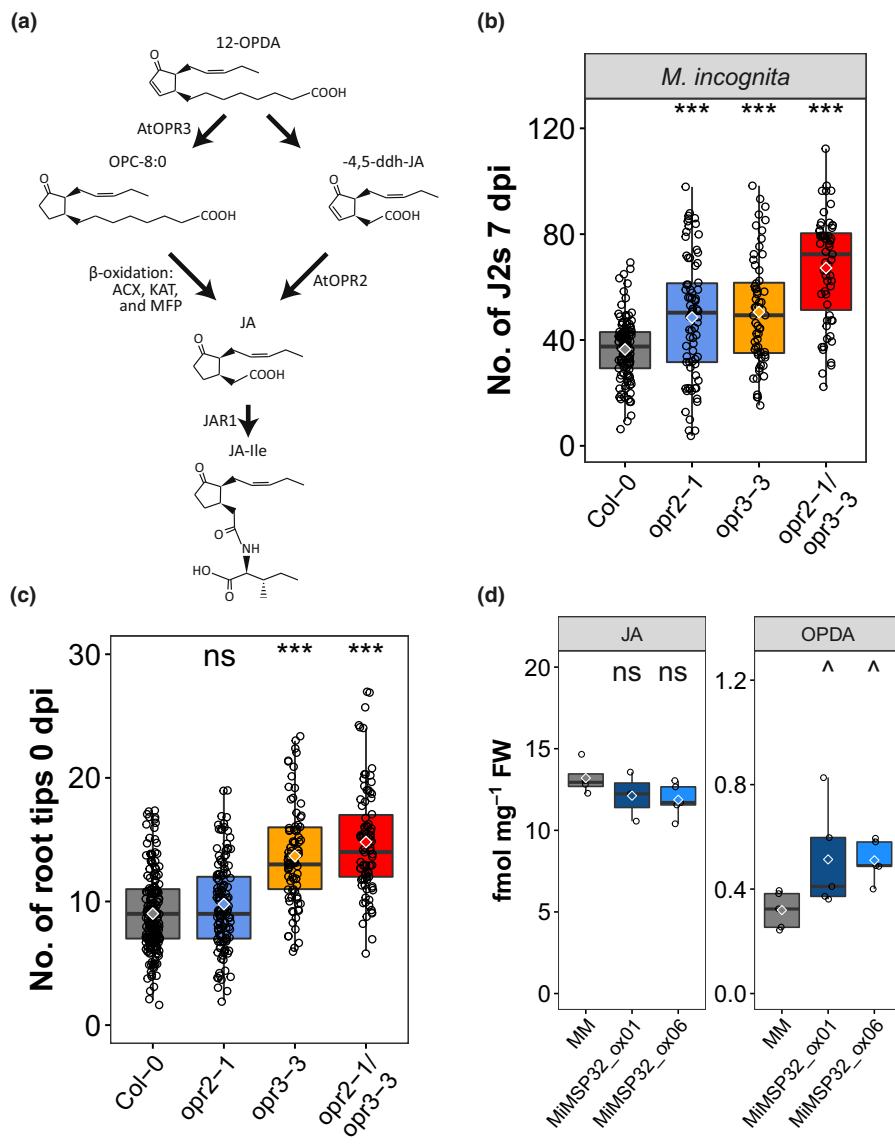
Fig. 6 12-oxophytodienoate reductase 2 (OPR2) regulates susceptibility to *Meloidogyne incognita* independently of OPR3. (a) Conversion of 12-oxophytodienoic acid (12-OPDA) into jasmonoyl-isoleucine by AtOPR3 and AtOPR2 as proposed by Chini *et al*. (2018). ACX, acyl-CoA oxidase; KAT, 3-ketoacyl-CoA thiolase; MFP, the multifunctional protein. (b) Number of acid fuchsin-stained *M. incognita* juveniles (J2s) in wild-type, opr2-1, opr3-3, or opr2-1/opr3-3 mutant plants at 7 d postinoculation (dpi). Data were collected in at least two independent experiments with a total $n \geq 27$ and combined for statistical analysis. (c) Number of root tips per genotype at the day of inoculation. (d) Hormone levels of jasmonic acid (JA) (i.e. total of JA and JA-Ile) and 12-OPDA (the total of the four different isomers, fmol mg^{-1} FW) in leaves of two independent tomato lines overexpressing MiMSP32 coding sequence (MiMSP32_ox01 and MiMSP32_ox06) without the predicted signal peptide for secretion and wild-type tomato plants (MM). All statistical differences were determined with a one-way ANOVA and a *post hoc* Tukey's HSD test. Boxplots represent the minimum, first quantile, median, third quantile, and maximum. The diamond shape represents the average value, and the circles represent all individual measurements. Asterisks indicate significant differences or between mutant or overexpression plants and wild-type plants: ***, $P < 0.001$; ^, $P < 0.10$; ns, not significant.

more research is needed to determine whether the sequence diversity observed in the cluster of paralogous genes to which MiMSP32 belongs mirrors adaptations in host targets, such as OPR2, involved in defense.

Our data from the Y2H screen, co-immunoprecipitation assays, and shifts in subcellular location suggest that MiMSP32 can interact with at least four unrelated host proteins. This could point at possible effector promiscuity, which has been observed for effectors of other plant pathogens. For instance, 32% of the bacterial type III effectors have multiple host targets with a similar molecular function, while 36% have multiple host targets with different molecular functions (Khan *et al.*, 2018). Bacterial type III effectors can target multiple unrelated host proteins located in different subcellular compartments allowing for spatial diversification in effector functions. Alternatively, promiscuous effectors also functionally diversify in time by targeting different host proteins at successive stages of the infection process (Thordal-Christensen *et al.*, 2018). Effector promiscuity can be based on the presence of multiple protein domains, providing different protein–protein interaction surfaces (Thordal-Christensen *et al.*, 2018). For example, the HopF1 effector in *Pseudomonas syringae* harbors two separately acting subdomains, shaped like the 'head' and the 'stalk' of a mushroom (Singer *et al.*, 2004). Smaller structural motifs within a single domain, such as the WY-domain fold, also facilitate binding of effectors to different host proteins (Franceschetti *et al.*, 2017). Within the protein sequence of MiMSP32, we have not found specific structural features, such as unusual charge distribution or a multiple-domain architecture, that could explain its binding to several unrelated host proteins. Nevertheless, evidence from earlier studies on nematode effectors indicates that effector promiscuity may also be a common theme in nematode–plant interactions. For instance, the effectors MiEFF1 of *M. incognita* (Truong *et al.*, 2021) and MgMO237 of *M. graminicola* (Chen *et al.*, 2018) interact with different unrelated host proteins. Likewise, the effector Hs25A01 from the beet cyst nematode *Heterodera schachtii* interacts with an Arabidopsis F-box-containing protein, a chalcone synthase, and the translation initiation factor eIF-2 b subunit (eIF-2bs; Pogorelko *et al.*, 2016). For the highly polyphagous root-knot

nematodes, effector promiscuity could be an efficient strategy enabling parasitism on a wide range of unrelated host plant species.

Our work establishes OPR2 as an important effector target of *M. incognita* for regulating the susceptibility of host plants. Upon nematode infection, OPR2 directs the root transcriptome toward biotic and abiotic stress responses. Here, we found 12 differentially regulated genes in the *opr2-1* mutant when compared to the wild-type Arabidopsis. Of the 12 differentially expressed genes, six have been functionally annotated, two of which can be specifically linked to processes known to occur in *M. incognita*-infected roots. As first, the differentially regulated *MAIL1* gene (At2g25010) is shown to be essential for maintaining correct cell division and differentiation in root apical meristems (Ühlken *et al.*, 2014). This could be a lead to investigate further as root-knot nematodes transform host cells into giant cells by bypassing cytokinesis in the mitotic cell division cycle (De Almeida & Gheysen, 2013). Furthermore, Arabidopsis *mail1* mutants show significant differentiation defects leading to disorganized growth of callus-like structures, which have evident similarities to the tumor-like galls formed around infection sites of root-knot nematodes (Olmo *et al.*, 2020). The second gene standing out in the list of OPR2-regulated transcripts, *MED8*, encodes a subunit of the Mediator complex involved in regulating JA-dependent defense responses to biotic and abiotic stresses (Kidd *et al.*, 2009; Zhang *et al.*, 2012; Li *et al.*, 2018). Further research using Arabidopsis mutants may show whether the genes differentially regulated in nematode-infected roots of the *opr2-1* mutant are causally related to host susceptibility, or whether they represent a secondary transcriptional fall-out of the catalytic activity of OPR2.

It has only recently been discovered that OPR2 catalyzes the conversion of 4,5-ddh-JA, a derivative of 12-OPDA, to JA (Chini *et al.*, 2018). Cytosolic OPR2 is positioned parallel to the peroxisomal JA biosynthesis pathway regulated by OPR3, which is thought to control the main route in the conversion of 12-OPDA into JA. Herein, OPR3 reduces 12-OPDA to 3-oxo-2(29 [Z]-pentenyl)-cyclopentane-1-octanoic acid (OPC:8), which is further converted through several ß-oxidation rounds into JA (Mussig *et al.*, 2000; Schaller *et al.*, 2000; Stintzi & Browse, 2000). Based on the mildly enhanced susceptibility to *M. incognita* of the *opr2-1* and *opr3-3* single mutants and the further increase in the susceptibility of the double-mutant *opr2-1/ opr3-3*, we conclude that both OPR2 and OPR3 are important and not operating redundantly in the complex hormonal regulation of host susceptibility to root-knot nematodes. This seems to contradict with earlier observations with the *opr3-1* mutant in Arabidopsis, which suggested that OPR3 is not required for host responses to root-knot nematodes (Gleason *et al.*, 2016). However, the *opr3-1* mutation is a conditional allele in the background on Arabidopsis ecotype Wassilewskija, while loss-of-function of *opr3-3* is unconditional in the background of Arabidopsis ecotype Columbia-0 (Chini *et al.*, 2018). Furthermore, Arabidopsis ecotypes exhibit significant quantitative variation in susceptibility to root-knot nematodes (Warmerdam *et al.*, 2018), which underlines that the genetic context of mutations can have a profound effect on observed plant phenotypes. Gleason *et al.* (2016) also conducted bioassays using the northern root-knot nematode *M. hapla*, which is only distantly related to *M.*

incognita and may be less sensitive to OPR3-dependent JA-mediated host responses. Notably, *M. hapla* was the only root-knot nematode species included in our comparative genome analyses that seem to lack an ortholog of MiMSP32.

The effector MiMSP32 may target host OPR2 to regulate the pool of 12-OPDA and downstream derivates, but targeting OPR2 alone is probably not sufficient to alter the accumulation of JA. Earlier work on Arabidopsis has shown that only in the background of the *opr3-3* mutant allele, OPR2 significantly affects the conversion of 4,5-didehydro-JA into JA and JA-Ile (Chini *et al.*, 2018). Our data show that OPR2 directs the transcriptome of nematode-infected roots toward abiotic and biotic responses, but this does not have a typical JA profile. Likewise, our tomato lines overexpressing MiMSP32 did not show a significant change in JA levels either, although we observed a slight increase in the level of 12-OPDA. The enhanced susceptibility of the single-mutant *opr2-1* and the MiMSP32 overexpressing plants to *M. incognita* may therefore not depend on JA signaling but could instead rely on the perception of 12-OPDA or other derivates. In line with this, Gleason *et al.* (2016) found that the Arabidopsis 12-OPDA receptor mutant *CYP20-3* is more susceptible to infections by root-knot nematodes, albeit it with a different species. Our data could thus add to the increasing evidence pointing at autonomous signaling functions of 12-OPDA distinct from JA in adaptive responses to biotic and abiotic stress (reviewed in Liu & Park, 2021). However, further research is needed to establish whether indeed MiMSP32 alters 12-OPDA levels in nematode-induced syncytia in an OPR2-dependent manner, and whether MiMSP32-enhanced susceptibility requires OPDA perception and signaling (Park *et al.*, 2013; Liu & Park, 2021).

In conclusion, *M. incognita* delivers the stylet-secreted effector MiMSP32 into host cell cytoplasm to modulate OPR2-dependent host defenses. Like root-knot nematodes, many wound-inducing pathogens and insects of plants are affected by oxylipin-dependent host defenses (Zhang *et al.*, 2017) and artificially manipulating the conversion of the 12-OPDA by 12-OPDA-reductases has been shown to alter susceptibility to multiple unrelated plant invaders (Scalschi *et al.*, 2015; Gleason *et al.*, 2016; Chini *et al.*, 2018). However, to the best of our knowledge, this study is the first to shed to light on a novel effector mechanism targeting this process to promote parasitism in plants.

Acknowledgements

to the equipment and technical support. Additionally, we would like to thank Unifarm of Wageningen University & Research for support with plant material and the Laboratory of Plant Breeding for support with plant transformations.

Competing interests

None declared.

Author contributions

AV, AF-T, PP, AG and GS designed the experiments. PP performed the initial positive selection analyses. AV performed most experiments and analyses. DRVR, CCS and HO helped to perform the laboratory experiments. KV cloned the effector constructs. EJS performed the FRET-FLIM and confocal experiments and helped to set up the Co-IPs. WT performed the AtOPR2 Co-IP. JJMS mapped the RNA-Seq reads. IFK performed the phytohormone measurements. MGS helped with the data analysis and interpretation. MQ supplied access to their Mi datasets and helped with the interpretation of results. AV, AG, MGS and GS wrote the paper.

ORCID

Anna Finkers-Tomczak https://orcid.org/0000-0002-4776-0619
Aska Goverse https://orcid.org/0000-0002-7399-8743
Iris F. Kappers https://orcid.org/0000-0003-3349-3473
Hein Overmars https://orcid.org/0000-0003-2461-4026
Pjotr Prins https://orcid.org/0000-0002-8021-9162
Michaël Quentin https://orcid.org/0000-0002-8030-1203
Erik J. Slootweg https://orcid.org/0000-0001-9935-7728
Geert Smant https://orcid.org/0000-0001-6094-8686
Joris J. M. Steenbrugge van https://orcid.org/0000-0002-9961-2538
Mark G. Sterken https://orcid.org/0000-0001-7119-6213
Ava Verhoeven https://orcid.org/0000-0001-9139-9050

Data availability

The RNA-Seq data that support the findings of this study are uploaded in ArrayExpress at https://www.ebi.ac.uk/arrayexpress/, reference number E-MTAB-11583. All other data are available from the corresponding author upon reasonable request.

References

Abad P, Gouzy J, Aury J-M, Castagnone-Sereno P, Danchin EGJ, Deleury E, Perfus-Barbeoch L, Anthouard V, Artiguenave F, Blok VC *et al.* 2008. Genome sequence of the metazoan plant–parasitic nematode *Meloidogyne incognita. Nature Biotechnology* 26: 909–915.

Abad P, Williamson VM. 2010. Plant nematode interaction: a sophisticated dialogue. *Advances in Botanical Research* 53: 147–192.

Alonso JM, Stepanova AN, Leisse TJ, Kim CJ, Chen H, Shinn P, Stevenson DK, Zimmerman J, Barajas P, Cheuk R *et al.* 2003. Genome-wide insertional mutagenesis of *Arabidopsis thaliana. Science* 301: 653–657.

Baskaran P, Jaleta TG, Streit A, Rödelsperger C. 2017. Duplications and positive selection drive the evolution of parasitism-associated gene families in the nematode *Strongyloides papillosus. Genome Biology and Evolution* 9: 790–801.

Bebber DP, Holmes T, Gurr SJ. 2014. The global spread of crop pests and pathogens. *Global Ecology and Biogeography* 23: 1398–1407.

Blanc-Mathieu R, Perfus-Barbeoch L, Aury J-M, Da Rocha M, Gouzy J, Sallet E, Martin-Jimenez C, Bailly-Bechet M, Castagnone-Sereno P, Flot J-F *et al.* 2017. Hybridization and polyploidy enable genomic plasticity without sex in the most devastating plant–parasitic nematodes. *PLoS Genetics* 13: e1006777.

Blum M, Chang H-Y, Chuguransky S, Grego T, Kandasaamy S, Mitchell A, Nuka G, Paysan-Lafosse T, Qureshi M, Raj S *et al.* 2021. The InterPro protein families and domains database: 20 years on. *Nucleic Acids Research* 49: D344–D354.

Carpentier J, Esquibet M, Fouville D, Manzanares-Dauleux MJ, Kerlan M-C, Grenier E. 2012. The evolution of the Gp-Rbp-1 gene in *Globodera pallida* includes multiple selective replacements. *Molecular Plant Pathology* 13: 546–555.

Chen J, Hu L, Sun L, Lin B, Huang K, Zhuo K, Liao J. 2018. A novel *Meloidogyne graminicola* effector, MgMO237, interacts with multiple host defence-related proteins to manipulate plant basal immunity and promote parasitism. *Molecular Plant Pathology* 19: 1942–1955.

Chini A, Monte I, Zamarreño AM, Hamberg M, Lassueur S, Reymond P, Weiss S, Stintzi A, Schaller A, Porzel A *et al.* 2018. An OPR3-independent pathway uses 4,5-didehydrojasmonate for jasmonate synthesis. *Nature Chemical Biology* 14: 171–178.

Da Rocha M, Bournaud C, Dazenière J, Thorpe P, Bailly-Bechet M, Pellegrin C, Péré A, Grynberg P, Perfus-Barbeoch L, Eves-van den Akker S *et al.* 2021. Genome expression dynamics reveal the parasitism regulatory landscape of the root-knot nematode *Meloidogyne incognita* and a promoter motif associated with effector genes. *Genes* 12: 771.

De Almeida EJ, Gheysen G. 2013. Nematode-induced endoreduplication in plant host cells: why and how? *Molecular Plant–Microbe Interactions* 26: 17–24.

Fan JW, Hu CL, Zhang LN, Li ZL, Zhao FK, Wang SH. 2015. Jasmonic acid mediates tomato's response to root knot nematodes. *Journal of Plant Growth Regulation* 34: 196–205.

Formstecher E, Aresta S, Collura V, Hamburger A, Meil A, Trehin A, Reverdy C, Betin V, Maire S, Brun C *et al.* 2005. Protein interaction mapping: a *Drosophila* case study. *Genome Research* 15: 376–384.

Franceschetti M, Maqbool A, Jiménez-Dalmaroni MJ, Pennington HG, Kamoun S, Banfield MJ. 2017. Effectors of filamentous plant pathogens: commonalities amid diversity. *Microbiology and Molecular Biology Reviews* 81: e00066-16.

Gao F, Chen C, Arab DA, Du Z, He Y, Ho SYW. 2019. EasyCodeML: a visual tool for analysis of selection using CodeML. *Ecology and Evolution* 9: 3891–3898.

Gheysen G, Mitchum MG. 2019. Phytoparasitic nematode control of plant hormone pathways. *Plant Physiology* 179: 1212–1226.

Gleason C, Leelarasamee N, Meldau D, Feussner I. 2016. OPDA has key role in regulating plant susceptibility to the root-knot nematode *Meloidogyne hapla* in Arabidopsis. *Frontiers in Plant Science* 7: 1565.

Huang G, Gao B, Maier T, Allen R, Davis EL, Baum TJ, Hussey RS. 2003. A profile of putative parasitism genes expressed in the esophageal gland cells of the root-knot nematode *Meloidogyne incognita. Molecular Plant–Microbe Interactions* 16: 376–381.

Hussey RS. 1989. Disease-inducing secretions of plant–parasitic nematodes. *Annual Review of Phytopathology* 27: 123–141.

Hussey RS, Barker KR. 1973. Comparison of methods of collecting inocula of *Meloidogyne* spp., including a new technique. *Plant Disease Reporter* 57: 1025–1028.

Khan M, Seto D, Subramaniam R, Desveaux D. 2018. Oh, the places they'll go! A survey of phytopathogen effectors and their host targets. *The Plant Journal* 93: 651–663.

Kidd BN, Edgar CI, Kumar KK, Aitken EA, Schenk PM, Manners JM, Kazan K. 2009. The mediator complex subunit PFT1 is a key regulator of jasmonate-dependent defense in *Arabidopsis. Plant Cell* 21: 2237–2252.

Kyndt T, Vieira P, Gheysen G, de Almeida-Engler J. 2013. Nematode feeding sites: unique organs in plant roots. *Planta* 238: 807–818.

Lamesch P, Berardini TZ, Li D, Swarbreck D, Wilks C, Sasidharan R, Muller R, Dreher K, Alexander DL, Garcia-Hernandez M *et al.* 2011. The

Arabidopsis Information Resource (TAIR): improved gene annotation and new tools. *Nucleic Acids Research* **40**: D1202–D1210.

Li C, Liu G, Xu C, Lee GI, Bauer P, Ling H-Q, Ganal MW, Howe GA. 2003. The tomato suppressor of prosystemin-mediated responses2 gene encodes a fatty acid desaturase required for the biosynthesis of jasmonic acid and the production of a systemic wound signal for defense gene expression. *Plant Cell* **15**: 1646–1661.

Li S, Ma J, Liu P. 2019. OPR3 is expressed in phloem cells and is vital for lateral root development in Arabidopsis. *Canadian Journal of Plant Science* **93**: 165–170.

Li X, Yang R, Chen H. 2018. The *Arabidopsis thaliana* mediator subunit MED8 regulates plant immunity to *Botrytis cinerea* through interacting with the basic helix–loop–helix (bHLH) transcription factor FAMA. *PLoS ONE* **13**: e0193458.

Liu W, Park S-W. 2021. 12-oxo-phytodienoic acid: a fuse and/or switch of plant growth and defense responses? *Frontiers in Plant Science* **12**: 724079.

Marchler-Bauer A, Bo Y, Han L, He J, Lanczycki CJ, Lu S, Chitsaz F, Derbyshire MK, Geer RC, Gonzales NR *et al.* 2016. CDD/SPARCLE: functional classification of proteins via subfamily domain architectures. *Nucleic Acids Research* **45**: D200–D203.

Mejias J, Truong NM, Abad P, Favery B, Quentin M. 2019. Plant proteins and processes targeted by parasitic nematode effectors. *Frontiers in Plant Science* **10**: 970.

Mitchum MG, Hussey RS, Baum TJ, Wang X, Elling AA, Wubben M, Davis EL. 2013. Nematode effector proteins: an emerging paradigm of parasitism. *New Phytologist* **199**: 879–894.

Mussig C, Biesgen C, Lisso J, Uwer U, Weiler EW, Altmann T. 2000. A novel stress-inducible 12-oxophytodienoate reductase from *Arabidopsis thaliana* provides a potential link between brassinosteroid-action and jasmonic-acid synthesis. *Journal of Plant Physiology* **157**: 143–152.

Nahar K, Kyndt T, de Vleesschauwer D, Höfte M, Gheysen G. 2011. The jasmonate pathway is a key player in systemically induced defense against root knot nematodes in rice. *Plant Physiology* **157**: 305–316.

Nguyen C-N, Perfus-Barbeoch L, Quentin M, Zhao J, Magliano M, Marteu N, Da Rocha M, Nottet N, Abad P, Favery B. 2018. A root-knot nematode small glycine and cysteine-rich secreted effector, MiSGCR1, is involved in plant parasitism. *New Phytologist* **217**: 687–699.

Olmo R, Cabrera J, Díaz-Manzano FE, Ruiz-Ferrer V, Barcala M, Ishida T, García A, Andrés MF, Ruiz-Lara S, Verdugo I *et al.* 2020. Root-knot nematodes induce gall formation by recruiting developmental pathways of post-embryonic organogenesis and regeneration to promote transient pluripotency. *New Phytologist* **227**: 200–215.

Opperman CH, Bird DM, Williamson VM, Rokhsar DS, Burke M, Cohn J, Cromer J, Diener S, Gajan J, Graham S. 2008. Sequence and genetic map of *Meloidogyne hapla*: a compact nematode genome for plant parasitism. *Proceedings of the National Academy of Sciences, USA* **105**: 14802–14807.

Ozalvo R, Cabrera J, Escobar C, Christensen SA, Borrego EJ, Kolomiets MV, Castresana C, Iberkleid I, Horowitz SB. 2014. Two closely related members of *Arabidopsis* 13-lipoxygenases (13-LOXs), LOX3 and LOX4, reveal distinct functions in response to plant–parasitic nematode infection. *Molecular Plant Pathology* **15**: 319–332.

Park S-W, Li W, Viehhauser A, He B, Kim S, Nilsson AK, Andersson MX, Kittle JD, Ambavaram MM, Luan S. 2013. Cyclophilin 20-3 relays a 12-oxo-phytodienoic acid signal during stress responsive regulation of cellular redox homeostasis. *Proceedings of the National Academy of Sciences, USA* **110**: 9559–9564.

Pogorelko G, Juvale PS, Rutter WB, Hewezi T, Hussey R, Davis EL, Mitchum MG, Baum TJ. 2016. A cyst nematode effector binds to diverse plant proteins, increases nematode susceptibility and affects root morphology. *Molecular Plant Pathology* **17**: 832–844.

Pokhare SS, Thorpe P, Hedley P, Morris J, Habash SS, Elashry A, Eves-van den Akker S, Grundler FMW, Jones JT. 2020. Signatures of adaptation to a monocot host in the plant–parasitic cyst nematode *Heterodera sacchari*. *The Plant Journal* **103**: 1263–1274.

Rain J-C, Selig L, De Reuse H, Battaglia V, Reverdy C, Simon S, Lenzen G, Petel F, Wojcik J, Schachter V *et al.* 2001. The protein–protein interaction map of *Helicobacter pylori*. *Nature* **409**: 211–215.

Riemann M, Haga K, Shimizu T, Okada K, Ando S, Mochizuki S, Nishizawa Y, Yamanouchi U, Nick P, Yano M *et al.* 2013. Identification of rice allene oxide cyclase mutants and the function of jasmonate for defence against *Magnaporthe oryzae*. *The Plant Journal* **74**: 226–238.

Robinson SJ, Tang LH, Mooney BAG, McKay SJ, Clarke WE, Links MG, Karcz S, Regan S, Wu Y-Y, Gruber MY *et al.* 2009. An archived activation tagged population of *Arabidopsis thaliana* to facilitate forward genetics approaches. *BMC Plant Biology* **9**: 101.

Sato K, Kadota Y, Gan P, Bino T, Uehara T, Yamaguchi K, Ichihashi Y, Maki N, Iwahori H, Suzuki T *et al.* 2018. High-quality genome sequence of the root-knot nematode *Meloidogyne arenaria* genotype A2-O. *Genome Announcements* **6**: e00519-18.

Scalschi L, Sanmartín M, Camañes G, Troncho P, Sánchez-Serrano JJ, García-Agustín P, Vicedo B. 2015. Silencing of *OPR3* in tomato reveals the role of OPDA in callose deposition during the activation of defense responses against *Botrytis cinerea*. *The Plant Journal* **81**: 304–315.

Schaller F, Biesgen C, Müssig C, Altmann T, Weiler EW. 2000. 12-Oxophytodienoate reductase 3 (OPR3) is the isoenzyme involved in jasmonate biosynthesis. *Planta* **210**: 979–984.

Scranton MA, Yee A, Park S-Y, Walling LL. 2012. Plant leucine aminopeptidases moonlight as molecular chaperones to alleviate stress-induced damage. *Journal of Biological Chemistry* **287**: 18408–18417.

Shi Q, Mao Z, Zhang X, Ling J, Lin R, Zhang X, Liu R, Wang Y, Yang Y, Cheng X *et al.* 2018a. The novel secreted *Meloidogyne incognita* effector MiISE6 targets the host nucleus and facilitates parasitism in Arabidopsis. *Frontiers in Plant Science* **9**: 252.

Shi Q, Mao Z, Zhang X, Zhang X, Wang Y, Ling J, Lin R, Li D, Kang X, Sun W. 2018b. A *Meloidogyne incognita* effector MiISE5 suppresses programmed cell death to promote parasitism in host plant. *Scientific Reports* **8**: 7256.

Shukla N, Yadav R, Kaur P, Rasmussen S, Goel S, Agarwal M, Jagannath A, Gupta R, Kumar A. 2018. Transcriptome analysis of root-knot nematode (*Meloidogyne incognita*)-infected tomato (*Solanum lycopersicum*) roots reveals complex gene expression profiles and metabolic networks of both host and nematode during susceptible and resistance responses. *Molecular Plant Pathology* **19**: 615–633.

Sijmons PC, Grundler FMW, von Mende N, Burrows PR, Wyss U. 1991. *Arabidopsis thaliana* as a new model host for plant–parasitic nematodes. *The Plant Journal* **1**: 245–254.

Singer AU, Desveaux D, Betts L, Chang JH, Nimchuk Z, Grant SR, Dangl JL, Sondek J. 2004. Crystal structures of the type III effector protein AvrPphF and its chaperone reveal residues required for plant pathogenesis. *Structure* **12**: 1669–1681.

Singh RR, Verstraeten B, Siddique S, Tegene AM, Tenhaken R, Frei M, Haeck A, Demeestere K, Pokhare S, Gheysen G *et al.* 2020. Ascorbate oxidation activates systemic defence against root-knot nematode *Meloidogyne graminicola* in rice. *Journal of Experimental Botany* **71**: 4271–4284.

Song H, Lin B, Huang Q, Sun T, Wang W, Liao J, Zhuo K. 2021. The *Meloidogyne javanica* effector Mj2G02 interferes with jasmonic acid signalling to suppress cell death and promote parasitism in Arabidopsis. *Molecular Plant Pathology* **22**: 1288–1301.

Stintzi A, Browse J. 2000. The Arabidopsis male-sterile mutant, *opr3*, lacks the 12-oxophytodienoic acid reductase required for jasmonate synthesis. *Proceedings of the National Academy of Sciences, USA* **97**: 10625–10630.

Szitenberg A, Salazar-Jaramillo L, Blok VC, Laetsch DR, Joseph S, Williamson VM, Blaxter ML, Lunt DH. 2017. Comparative genomics of apomictic root-knot nematodes: hybridization, ploidy, and dynamic genome change. *Genome Biology and Evolution* **9**: 2844–2861.

Thordal-Christensen H, Birch PRJ, Spanu PD, Panstruga R. 2018. Why did filamentous plant pathogens evolve the potential to secrete hundreds of effectors to enable disease? *Molecular Plant Pathology* **19**: 781–785.

Truong NM, Chen Y, Mejias J, Soulé S, Mulet K, Jaouannet M, Jaubert-Possamai S, Sawa S, Abad P, Favery B *et al.* 2021. The *Meloidogyne incognita* nuclear effector MiEFF1 interacts with *Arabidopsis* cytosolic glyceraldehyde-3-phosphate dehydrogenases to promote parasitism. *Frontiers in Plant Science* **12**: 641480.

Ühlken C, Horvath B, Stadler R, Sauer N, Weingartner M. 2014. MAIN-LIKE 1 is a crucial factor for correct cell division and differentiation in *Arabidopsis thaliana*. *The Plant Journal* **78**: 107–120.

Vinutha HP, Poornima B, Sagar BM. 2018. Detection of outliers using interquartile range technique from intrusion dataset. In: Satapathy SC, Tavares

JMRS, Bhateja V, Mohanty JR, eds. *Information and decision sciences. Advances in intelligent systems and computing, vol. 701.* Singapore City, Singapore: Springer, 511–518.

Wang G, Hu C, Zhou J, Liu Y, Cai J, Pan C, Wang Y, Wu X, Shi K, Xia X et al. 2019. Systemic root-shoot signaling drives jasmonate-based root defense against nematodes. *Current Biology* **29**: 3430–3438.

Warmerdam S, Sterken MG, van Schaik C, Oortwijn ME, Sukarta OC, Lozano-Torres JL, Dicke M, Helder J, Kammenga JE, Goverse A. 2018. Genome-wide association mapping of the architecture of susceptibility to the root-knot nematode *Meloidogyne incognita* in *Arabidopsis thaliana. New Phytologist* **218**: 724–737.

Wickham H. 2016. GGPLOT2: *elegant graphics for data analysis.* New York, NY, USA: Springer-Verlag.

Williamson VM, Gleason CA. 2003. Plant–nematode interactions. *Current Opinion in Plant Biology* **6**: 327–333.

Wyss U, Grundler FMW. 1992. Feeding behavior of sedentary plant parasitic nematodes. *Netherlands Journal of Plant Pathology* **98**: 165–173.

Yang Z. 1997. PAML: a program package for phylogenetic analysis by maximum likelihood. *Bioinformatics* **13**: 555–556.

Yang Z. 2007. PAML 4: phylogenetic analysis by maximum likelihood. *Molecular Biology and Evolution* **24**: 1586–1591.

Yang Z, Bielawski JP. 2000. Statistical methods for detecting molecular adaptation. *Trends in Ecology & Evolution* **15**: 496–503.

Zhang L, Zhang F, Melotto M, Yao J, He SY. 2017. Jasmonate signaling and manipulation by pathogens and insects. *Journal of Experimental Botany* **68**: 1371–1385.

Zhang X, Wang C, Zhang Y, Sun Y, Mou Z. 2012. The *Arabidopsis* mediator complex subunit16 positively regulates salicylate-mediated systemic acquired resistance and jasmonate/ethylene-induced defense pathways. *Plant Cell* **24**: 4294–4309.

Supporting Information

Additional Supporting Information may be found online in the Supporting Information section at the end of the article.

Fig. S1 Characteristics of tomato plants overexpressing MiMSP32 or the MiMSP32 hairpin construct.

Fig. S2 Confirmation of Arabidopsis T-DNA insertion lines *ala1-1*, *ala1-2*, *tppII-2*, and *opr2-1*.

Fig. S3 Confirmation of Arabidopsis T-DNA insertion lines *opr3-3* and *opr2-1/opr3-3*.

Fig. S4 MiMSP31 and MiMSP32 and three paralogous genes in the genome of *Meloidogyne incognita*.

Fig. S5 Position of yeast two-hybrid clone inserts interacting with MiMSP32 relative to the whole gene sequence of the six putative host targets.

Fig. S6 MiMSP32 interacts specifically with five host proteins.

Fig. S7 MiMSP32 co-localizes with four host proteins.

Fig. S8 RNA-Seq transcripts affected by time and treatments.

Fig. S9 Expression of jasmonic acid biosynthesis associated genes (KEGG module M00113) in nematode-infected roots of the *opr2-1* mutant and wild-type Col-0 plants over time.

Methods S1 Construction of MiMSP32^{-sp}-derived plasmids for stable transformation of tomato plants.

Methods S2 Transformation of tomato plants.

Methods S3 Transient expression assays and total protein extraction.

Methods S4 Quantitative PCR.

Methods S5 Construction of MiMSP32^{-sp}-derived plasmids for transient expression in *Nicotiana benthamiana*.

Methods S6 Construction of plasmids encoding host protein fragments for transient expression in *Nicotiana benthamiana*.

Methods S7 Whole transcriptome analysis by RNA-Seq.

Methods S8 Phytohormone measurements in MiMSP32_ox tomato plants.

Table S1 Primers used in this study.

Table S2 All estimates of parameters for the different models of evolution for the 27 MiMSPs.

Table S3 Summary statistics of the yeast two-hybrid screen results.

Table S4 Yeast two-hybrid screen identified 11 probable candidate interactors of MiMSP32, of which six with a high confidence in the interaction.

Table S5 Overview of the six tomato proteins interacting with MiMSP32 in yeast two-hybrid.

Table S6 Physiochemical protein characteristics for MiMSP32^{-sp} and the six selected interaction domains of the six putative tomato host targets as predicted by ExPASy.

Table S7 RNA-Seq mapping statistics.

Table S8 RNA-Seq differentially regulated genes between *opr2-1* mutant plants and Col-0 wild-type plants, based on an interaction model for plant line and *Meloidogyne incognita* infection.

Table S9 Details of the 13 differentially regulated genes between nematode-infected roots of the Arabidopsis *opr2-1* mutant and wild-type Col-0 plants as extracted from the TAIR database.

Please note: Wiley is not responsible for the content or functionality of any Supporting Information supplied by the authors. Any queries (other than missing material) should be directed to the *New Phytologist* Central Office.